Studies of the measurement of respirable coal dusts and diesel particulate matter

INSTITUTE OF PHYSICS PUBLISHING MEASUREMENT SCIENCE AND TECHNOLOGY
Meas. Sci. Technol. **13** (2002) 365–374 PII: S0957-0233(02)27715-2

Studies of the measurement of respirable coal dusts and diesel particulate matter

Charles D Litton

Pittsburgh Research Laboratory, National Institute for Occupational Safety and Health, PO Box 18070, Cochrans Mill Road, Pittsburgh, PA 15236, USA

E-mail: chl3@cdc.gov

Received 8 August 2001, in final form 24 October 2001, accepted for publication 5 November 2001
Published 8 February 2002
Online at stacks.iop.org/MST/13/365

Abstract
Experiments were conducted to determine the optical scattering properties of respirable coal dusts and diesel particulate matter (DPM) at discrete angles in the forward direction and at light source wavelengths of 632.8 and 635 nm. In addition to the scattering data, simultaneous measurements were made of the total mass concentration of dust, DPM or mixtures of the two, and the responses of a unipolar ion chamber and a simpler, more common bipolar ion chamber typical of residential smoke detectors. The results of these experiments indicate, for respirable coal dusts, that the intensity per unit mass concentration at discrete angles in the range of 15°–30° varies linearly with mass concentration independent of the volatility of the dust, but that at larger scattering angles, intensities per unit mass concentration are affected by dust volatility. For DPM, the intensities per unit mass concentration are significantly lower. The results also indicate that the ion chambers respond significantly to DPM while there is no response to respirable coal dust, and that when mixtures of the two are present, the ion chambers respond to the DPM mass fraction only. In addition, it was found that the angular intensity distribution for respirable dusts is adequately described by classical Mie scattering theory, while for DPM classical Mie scattering is inadequate, and treatment of the particles as fractal-like aggregates yields much better agreement with the experimental data. This paper describes the experiments and their results.

Keywords: light scattering, combustion aerosols, ions, laser diodes, ionization chambers, environmental monitoring, respirable dusts

(Some figures in this article are in colour only in the electronic version)

1. Introduction

1.1. Overview

In the initial stages of this research, the objective was to study, both theoretically and experimentally, the angular distribution of scattered light from a polydisperse system of respirable coal dust particles as a function of size distribution, volatility and wavelength of incident radiation. As the research progressed, a need was identified to be able to simultaneously measure concentrations of diesel particulate matter (DPM) and respirable coal dust in atmospheres containing both constituents. This paper addresses and assesses the potential of light scattering and, as it evolved, ion chamber response and/or combinations of the two, as they apply to these measurement problems.

1.2. Respirable dust and DPM

Coal workers' pneumoconiosis (CWP), or 'black lung', is a major health problem resulting from coal miners' prolonged exposure to respirable coal dusts, dusts with mass mean diameters typically less than 10 μm. To reduce this problem and provide protection against the occurrence of CWP, current coal mining regulations require that exposure of personnel to respirable coal mine dusts be limited to an 8 h time-weighted average that does not exceed 2.0 mg m^{-3} [1]. The standard measurement technique for this determination is continuous sampling of the mine atmosphere through a small, 10 mm cyclone at a nominal flow rate of 2.0 l min^{-1}. The cyclone operating at the specified flow rate is designed to simulate

the penetration of respirable dust into the human lung. Those particles that make their way through the cyclone are deposited onto a preweighed filter. The filter is then weighed at the end of an 8 h sampling period and the time-weighted mass concentration, m_0, in mg m^{-3}, determined from the expression

$$m_0 = m_F/(Q_0 t) \tag{1}$$

where m_F is the total mass of dust deposited on the filter (mg), Q_0 is the flow rate (0.002 m^3 min^{-1}), and t is the total sampling time in minutes.

While this is the generally accepted standard technique for determination of respirable dust concentrations, such determinations are cumbersome and time-consuming to complete. As a result, alternative approaches to the measurement of respirable dust concentrations are being studied for their adequacy and accuracy.

In addition, many mines use diesels extensively, and the use of diesels makes the measurement more complex for a number of reasons. First, the particles deposited on a filter are due both to DPM and respirable dust, and there is no simple technique for determining their relative contributions to the total mass deposited. Second, there are significant and different adverse health effects related to DPM (DPM is a suspected carcinogen), with the result that the maximum allowable time-weighted average concentration for DPM is a factor of 10 lower than that for respirable dust. Consequently, it is important not only to be able to determine the airborne mass concentrations of both DPM and respirable dust, but DPM concentrations need to be measured at significantly lower concentrations. For DPM, the current standard is NIOSH 5040 [2], which is based upon the determination of elemental carbon and organic carbon. However, the chemical composition of DPM may contain significant components of volatile organic compounds, as great as 55–60% [3], so that under some conditions of diesel operation, these standard determinations may not be valid.

1.3. Current techniques

Various techniques have been proposed and studied to address these measurement problems. One technique involves the measurement of the pressure drop across the filter onto which the particles are deposited [4], an application of D'Arcy's law for flow through a porous bed of particles, where the pressure drop across the particle bed, or layer, is a function of the particle concentration and size. While this technique appears to work reasonably well for samples that contain no DPM, the presence of even minute quantities of DPM renders the technique unreliable. Even for pure respirable dust samples, significant variations in the pressure drop per unit mass, due most probably to differing particle size distributions, can occur, often resulting in meaningless or skewed measurements.

Aerodynamic separation of DPM and respirable dusts [5] has shown that, typically, particles with diameters less than about 0.7 μm are from diesels while larger particles are due to respirable dusts, although in the region of particle diameters between 0.7 and 1.0 μm overlap between the two sources of particles often occurs that makes the determination of individual mass concentrations difficult. In addition, even simple aerodynamic separation techniques require not only very precise flow control but also result in additional filter mass measurements that are even more cumbersome and time-consuming to complete.

Continuous, real-time mass measurements using such devices as the tapered element oscillating microbalance (TEOM) [6] have also been proposed for monitoring of either DPM or respirable dusts, but are incapable of separating the two when both exist simultaneously. In this technique, a filter is mounted onto what amounts to a hollow tuning fork vibrating at a fixed frequency. Particles in the flow through this filter are deposited on the filter, increasing the filter mass. As the filter mass increases, the frequency of vibration decreases proportionally. While the extension of these continuous, real-time measurement techniques to individual personnel monitoring is feasible, the cost of such devices becomes a major concern.

1.4. Light scattering

The use of light scattering as a technique for measurement of aerosol and/or respirable dust concentrations is not new. Light scattering is attractive as a measurement technique because it is simple and generally inexpensive to implement. Currently there exist several commercially available instruments that utilize this technique, although significant differences exist among the various instruments. Some utilize angular intensities measured at a forward angle of around 12°, while some measure the intensity in the angular range of 16°–18°. Another light-scattering instrument measures the intensity over the angular range 45°–90°, with a maximum sensitivity at around 60°. Most use a light source with a wavelength in the vicinity of 900 nm. However, depending upon the combination of light source wavelength and measurement angle, some of these devices become very sensitive to particle size distributions, or average particle diameters, while some become sensitive to the chemical composition of the scattering particles. These effects can introduce unacceptable errors in the determination of mass concentration. In addition, a major criticism of the light scattering technique is that it is not a direct mass measurement. Rather, mass concentrations are inferred based upon some method of calibration, yet because of particle size, chemical composition, or some other effect, the calibration may not be sufficient to yield accurate determinations of mass concentration over a broad range of aerosol or respirable dust characteristics.

Because of these potential difficulties, a portion of this research is to determine, if possible, those combinations of scattering angle and light source wavelength where the effects of particle size and chemical composition are either negligible or minimal, especially as this may pertain to the measurement of respirable dust concentrations. A major tool used to make these determinations is a robust Mie scattering algorithm [7] modified to account for a wide range of particle size distributions, chemical compositions via the index of refraction, and light source wavelengths. For DPM, previous studies [8] have shown that the Mie theory is not adequate to describe their angular scattering properties, and that treatment of these particles as fractal-like aggregates is more appropriate, yielding much better agreement with the experimental data. In general, the scattering properties of combustion aerosols are best described by treating the aerosol as a system of

fractal-like aggregates (see, for instance, [9, 10]). For a more comprehensive treatment of light scattering by fractal aggregates, the reader is referred to the review article by Sorensen [11].

1.5. Ion chambers

Ion chambers in the form of ionization-type smoke detectors have been used routinely as early-warning fire sensors since the mid 1970s. Typically, the source of ions in these types of ion chambers is a very low level radioactive source of americium-241 (Am-241). Am-241 decays via the emission of alpha particles (He nuclei) and as these particles traverse the air space between two electrodes, both positive and negative ions are created. The positive ions drift to the negative electrode while the negative ions drift to the positive electrode. This separation of ions, coupled with the geometry of the chamber, creates a space charge that distorts the electric field and electric potential within the ion chamber. A third, floating electrode is generally located between the positive and negative electrode at a position where the electric potential reaches its maximum distortion, and the potential at this electrode is continuously measured. When DPM, and possibly respirable coal dust, enters the air space between the electrodes, the positive and negative ions rapidly attach to the aerosol particles, depleting the ion concentrations, which, in turn, reduces the distortion of the electric potential causing the potential at the floating electrode to increase.

Very early in the development of these chambers it was found that such detectors are more sensitive to aerosols produced from flaming combustion than they are to aerosols produced from smouldering combustion. The reason for this difference in sensitivity is the result of two factors. First, the response of an ionization chamber to the presence of an aerosol at low concentrations varies directly with the product of number mean particle diameter, d_G, and number concentration, n_0, or $d_G n_0$ [15]. Consequently, for aerosol sources that produce large numbers of very small particles, the sensitivity will be high. Second, when small particles form aggregates of much larger extent, high sensitivity will also result for low to moderate concentrations of these larger aggregates.

Previous research results [8] indicated that the primary particle diameter for DPM is in the range of 25 nm and that these primary particles aggregate to form filaments of irregular shape with a typical radius of gyration, R_G, in the range of 450–500 nm. In addition, these aggregates were typically composed of about 1500 individual primary particles. If it is assumed that each primary particle has a density of 1.5 g cm^{-3}, then a simple calculation indicates that the mass of one aggregate particle containing 1500 primary particles is of the order of 2×10^{-14} g, and that the number of aggregates per cm^3 necessary to achieve a mass concentration of 2×10^{-9} g cm^{-3} (2 mg m^{-3}) is 1×10^5. If the number mean particle diameter is taken to be twice the radius of gyration, then the product, $d_G n_0$, is in the range of 9–10. Similarly, if it is assumed that an average respirable coal dust particle has a diameter of 4 μm and a density of 1.35 g cm^{-3}, then the number of particles necessary to produce the same mass concentration is about 50, so that the product $d_G n_0$ is about 0.02. Since the sensitivity of an ion chamber varies directly with $d_G n_0$, this means that the ion chamber is about 500 times more sensitive to DPM than to respirable coal dust. These numbers indicate that an ion chamber should be so much more sensitive to DPM that any contribution from respirable coal dust would be negligible. To test this hypothesis, the response of a typical ion chamber was measured for DPM, respirable coal dust and mixtures of the two. The results of these experiments are presented in section 3.

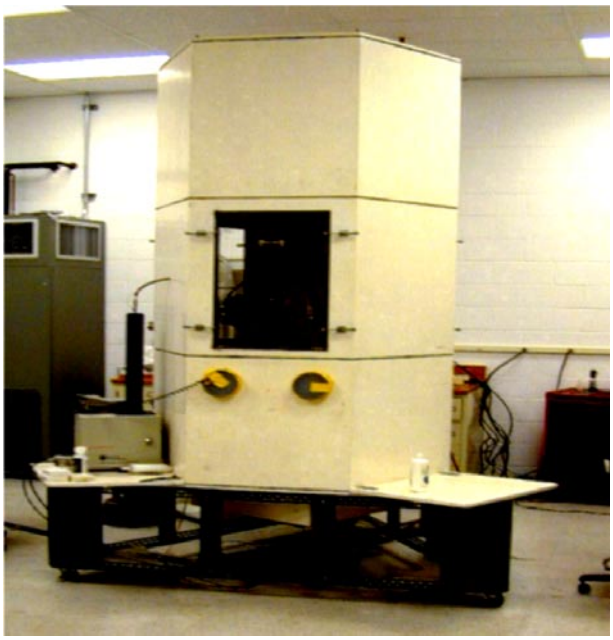

Figure 1. Photograph of the dust box used in the experiments.

2. Experiment

The experimental system in which the tests were conducted, known generically as a 'dust box' is shown in figure 1 and described in greater detail in [12]. Briefly, dusts or aerosols are dispersed near the top of the dust box, allowed to mix thoroughly and then fall via gravity coupled with a small, imposed flow. Samples of either respirable coal dust or DPM are extracted through 10 mm cyclones near the bottom of the dust box at nominal flow rates of 2 l min^{-1} and flowed to the various measuring devices. In this configuration, data were acquired for various respirable coal dusts, DPM from the exhaust of the diesel generator under different load conditions, and mixtures of respirable coal dust and DPM.

2.1. Measuring devices

During the experiments a TEOM, described previously [6], was used to continuously measure the mass concentrations of DPM or respirable coal dusts. For light scattering, two different devices were used. The first scattering module, shown schematically in figure 2, consists of two right circular discs, each with a diameter of 10.16 cm and a height of 2.54 cm, with their centres separated a distance of 15.2 cm. A small HeNe laser operating at a wavelength of 632.8 nm with an output power level of 3 mW and a beam diameter of 1.0 mm was attached at one end and the beam allowed to traverse the centreline of the two discs. For all of the experiments, angular

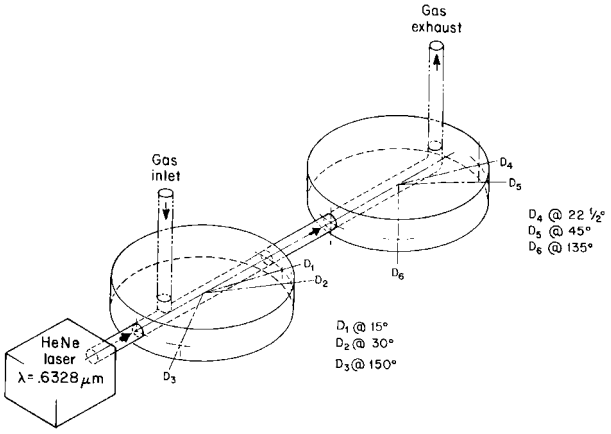

Figure 2. Schematic of the first light scattering module using a HeNe laser at $\lambda = 632.8$ nm as the light source. In this chamber, aerosols are flowed along the direction of the laser beam.

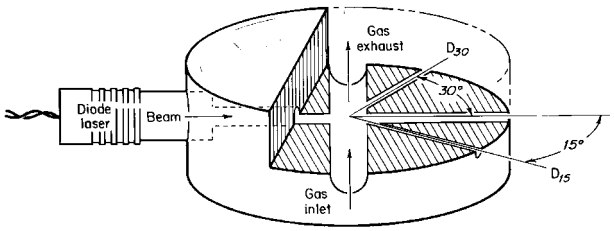

Figure 3. Schematic of the second light scattering module using a laser diode at $\lambda = 635$ nm as the light source. In this chamber, aerosols are flowed through the scattering module normal to the direction of the diode laser beam.

intensities were measured at angles of 15° and 30° within the first disc and at angles of 22.5° and 45° within the second disc using four PIN-125DP/L silicon photodiode detectors with measured responsivities of 0.24 A W^{-1} at $\lambda = 632.8$ nm. The active surface of each photodiode was located 4.45 cm from the centre of the respective discs with the air space between the photodiodes and the central scattering volume cylindrical in shape with a diameter of 0.25 cm. For this scattering module, aerosols were flowed into the module and then along the path of the light beam. In presentation of the data, all measurements made using this module are denoted with subscript '1'. For instance, I_1 [15] denotes the intensity measured at 15° using scattering module 1.

For the purposes of future development, a second, simpler prototype scattering module was fabricated for test and evaluation. This second scattering module, shown schematically in figure 3, is a right circular disc with a diameter of 7.62 cm and a height of 2.54 cm. Two PIN-125DP/L photodiodes, identical in physical configuration to those of the first module but with responsivities of 0.39 A W^{-1} at $\lambda = 635$ nm, with their active surfaces located 3.2 cm from the disc centre, were used to measure the angular intensities at 15° and 30°. The air space between the photodiode and central scattering volume is cylindrical with a diameter of 0.20 cm. For this second module, a small laser diode operating at a wavelength of 635 nm and an output power level of 5–6 mW was used as the light source. For this light source, the beam was brought to an approximate focus in the centre of the scattering volume with a spot diameter of about 2 mm. In addition, for

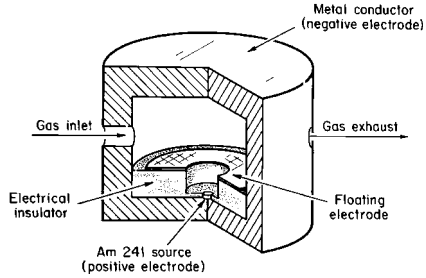

Figure 4. A schematic of the first, bipolar ion chamber utilizing a floating electrode for detection and measurement of aerosols.

this module, the aerosols were flowed through the scattering volume at right angles to the direction of the laser diode beam, rather than along the direction of the beam as was done in the first module. Data obtained using this module are denoted with a subscript '2'.

For both scattering modules, the actual scattering volumes vary inversely with the sine of the scattering angle, so that as the angle increases, the scattering volume decreases. Assuming the scattering volumes to be defined by the beam diameter of the light source, d_{BEAM}, and the diameters of the cylindrical light paths from the beam to the detectors, d_{DET}, then the volumes at each angle may be calculated approximately from the expression

$$V(\theta) = (\pi/4) d_{\mathrm{DET}}^2 d_{\mathrm{BEAM}} / \sin(\theta). \qquad (2)$$

The bipolar ion chamber used in these experiments, typical of ion chambers found in ionization-type smoke detectors, is shown schematically in figure 4. In this chamber, a 2.0 mm diameter source of Am-241 with an activity of 0.80 μCi and face coated with a 2.0 μm thick Pd foil, is placed in the centre of the base of a small cylindrical cavity with a diameter of 0.95 cm and height of 0.45 cm. At a distance of 0.45 cm from the source surface, the chamber abruptly expands to form a larger cylinder with a diameter of 3.25 cm. At the top of the larger cylinder is the negative electrode with its surface located a total distance of 1.90 cm from the surface of the source, which also serves as the positive electrode. Within these two volumes, both positive and negative air ions are created so that the chamber is referred to as a bipolar chamber. At the top of the smaller cylinder (0.45 cm distant from the source) is a floating conductor used to measure the electric potential at this plane in the chamber. The position of this floating conductor corresponds approximately to the plane of maximum distortion of the potential within the chamber. When operated at the standard voltage of 9.0 V, the potential at this plane is generally in the range of 3.4–3.9 V, a result of distortion of the electric field and potential due to space charge effects. If there were no source in the chamber, a simple electrostatic analysis indicates that the potential at this plane would be ~6.85 V. The difference, 2.95–3.45 V, represents the dynamic range for the potential at this position. When aerosols enter the chamber, they deplete the ions via attachment, and cause the potential to increase. Normally, aerosols enter the chamber via diffusion or via convective air flows, but for these experiments, the chamber was modified so that aerosols could be flowed through the chamber, entering and leaving at two opposite points halfway between the floating conductor and the top, negative electrode.

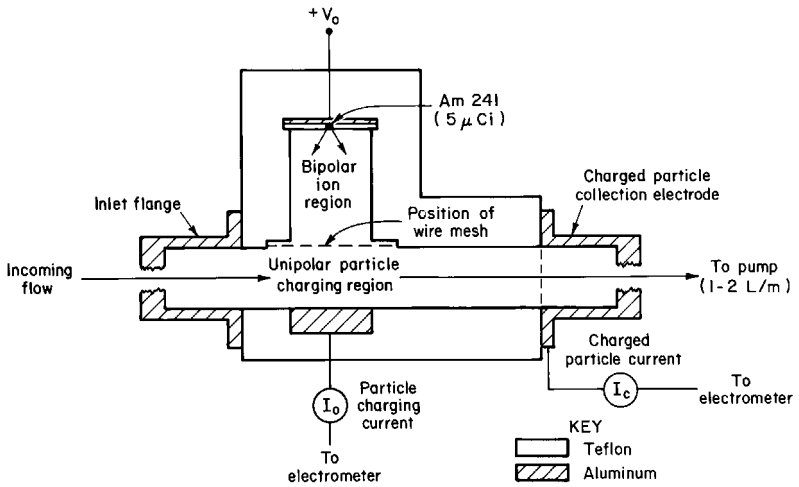

Figure 5. Schematic of the second, unipolar ion chamber for detection and measurement of aerosols, along with capability for estimate of average aerosol diameter and aerosol number concentration.

In addition to the above standard ion chamber, a second ion chamber in which a region of unipolar positive ions is created was also used. A schematic diagram of this chamber is shown in figure 5. The primary difference between this chamber and the bipolar chamber is that in this chamber aerosols are flowed through a region of unipolar ions where they acquire charge via the process of diffusion charging. The charged aerosol then flows out of the chamber into a third, collection electrode producing a current that depends upon the average charge per particle and the number concentration of particles. By continuously measuring the reduction of ion current within the unipolar ion region and the charged particle current at the collection electrode, it is possible to get an estimate of the average diameter and number concentration of the flowing aerosol. For this chamber, the ratio of primary charging current, I, when an aerosol is present to the initial, steady-state current, I_0, when no aerosol is present is denoted by the parameter, η, which depends upon the number mean diameter and number concentration via the expression

$$\eta = (1/\kappa_0 d_G n_0)[1 - \exp(-\kappa_0 d_G n_0)] \tag{3}$$

where κ_0 is a chamber constant with an empirically determined value of 0.0217 cm^2.

For values of $\eta \geqslant 0.90$, a Taylor series expansion of equation (3) yields

$$1 - \eta = \tfrac{1}{2}\kappa_0 d_G n_0. \tag{4}$$

The charged particle current at the collection electrode, amplified and converted to a voltage, V_C, depends upon η, d_G, and the flow, Q_0, via the expression

$$V_C = 0.0325 Q_0 (1 - \eta) \ln[1 + (2.3 \times 10^7 d_G / Q_0)] \tag{5}$$

where Q_0 is the flow rate in cm^3 s^{-1}, held constant at 33.3 cm^3 s^{-1} (2 l min^{-1}).

Measurements of V_C and η and use of equation (5) leads to a determination of d_G. Equation (4) can then be used to determine the number concentration, n_0.

3. Results and analysis

3.1. Respirable coal dust

Coal, and respirable coal dust produced during the mining process, is not a simple organic material with a well-defined and constant chemical composition and structure. Rather, the composition of various coals varies dramatically, from anthracite coal which contains mostly carbon and a low volatility in the range of 4% to a form of coal called gilsonite that contains less carbon and a volatility in the range of 85%. The index of refraction, $m = n - ik$, and, in particular, the extinction coefficient, k, are strong functions of both coal volatility and wavelength of incident radiation. For instance, for coal with a volatility of 5%, the value of k at a wavelength of 632.8 nm is about 0.41, while for coal with a volatility of 40%, k has a value of about 0.05. If the wavelength is increased to 900 nm, the corresponding respective values decrease to 0.18 and 0.02. The real component, n, tends to vary slightly with coal volatility, but the variation with wavelength is negligible throughout the visible and near-infrared regions of the spectrum. Generally, the data available for n and k are given in terms of the atomic hydrogen to carbon ratio, H/C, and it is necessary to convert measured values of coal volatility to H/C values. Figure 6 is a plot of the atomic H/C ratio as a function of the per cent volatility for a wide range of coals. These data were obtained from the literature [13] and from proximate and ultimate analyses of different coals obtained over the years at our laboratory. A linear regression of these data yields the following empirical expression for H/C as a function of volatility

$$\mathrm{H/C} = 1.23\,(\%\ \text{volatility}/100)^{0.4125}. \tag{6}$$

The variation of k with the ratio H/C and with λ is found to follow the empirical expression

$$k = k_0 \mathrm{e}^{-3\lambda} \tag{7}$$

where λ is the wavelength of incident light in μm and

$$k_0 = 5.35 - 7.25(\mathrm{H/C}) \qquad \text{for} \quad \mathrm{H/C} \leqslant 0.60$$
$$k_0 = 15\mathrm{e}^{-4.5(\mathrm{H/C})} \qquad \text{for} \quad \mathrm{H/C} > 0.60.$$

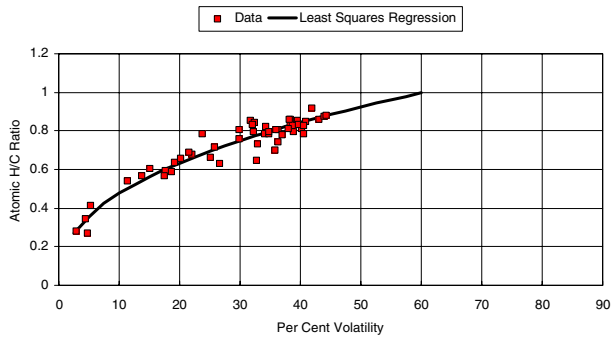

Figure 6. The dependence of atomic H/C ratio on the per cent volatility of different respirable coal dusts.

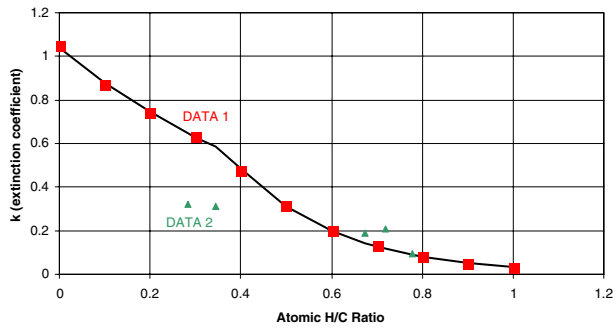

Figure 7. The extinction coefficient, k, (imaginary component of the complex index of refraction) as a function of the atomic H/C ratio. Data 1 from [14]; data 2 from [13].

Figure 7 is a plot of k versus the atomic H/C ratio at a wavelength of 546 nm (0.546 μm) using the above expressions, along with data from the literature [13, 14] obtained at this wavelength. An additional analysis of the literature data indicates that n depends upon the H/C ratio via the expression

$$n = 2.17 - 0.51(\mathrm{H/C}). \tag{8}$$

The use of these expressions then allows for the determination of the index of refraction, m, for any coal, from a simple measurement of coal volatility. These expressions were then incorporated into a robust Mie scattering algorithm [7] so that the effects of volatility on the angular intensity distribution of scattered light could be determined. In addition to the effects of coal volatility, the algorithm was modified to obtain the integral average angular intensities over a distribution of particle sizes. For the purposes of this work, the size distribution was assumed to be log-normal and different distributions could be input to the program by specifying the mass mean diameter, d_M, and the geometric standard deviation of the distribution, σ. In addition to size distribution parameters and coal volatility, other inputs included the wavelength of incident radiation, λ, and the angular increment, $\Delta\theta$, which could be varied in increments of 1°, 3°, 5°, and up to increments of 90°, so long as increments in excess of 5° are divisible by 5.

Over the years, several field investigations to determine particle size distributions of respirable dust in underground coal mines have been conducted. Three extensive surveys are summarized in [5], where approximately 110 different distributions are tabulated, encompassing several mines, as

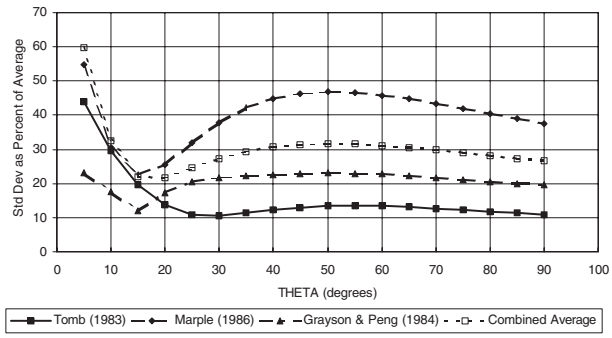

Figure 8. The standard deviation, expressed as a per cent of the mean intensity, as a function of scattering angle for respirable coal dust size distributions reported in the literature, using $\lambda = 632.8$ nm and averaged over the range of volatilities from 15 to 45%.

well as different locations within mines. Within these data, values of d_M vary over the range of 2.7–10 μm (average about 6.0 μm) while values of σ vary over the range of 1.7–3.2 (average about 2.35). Most of the data contain little information on the volatility of the coal, but from the names of the mines and coal seams listed, the coal volatility could be estimated to lie in the range of 15–40%. These data indicate the diversity of particle size distributions of respirable dust that can exist within underground mines. As should be expected, when the angular intensities are calculated individually using the Mie scattering algorithm, for these size distributions at a fixed volatility and wavelength differences result. To assess the magnitude of these differences, the arithmetic means and standard deviations of the calculated intensities at angles from 5°–90°, in increments of 5°, at an average volatility of 30% and a wavelength of 632.8 nm were computed and the standard deviation then expressed as a percentage of the arithmetic mean. The results for each data set, and for the three data sets combined, are shown in figure 8. Differences exist between the different data sets, but all three, along with the combined average, show that the angular region corresponding to the minimum variation lies in the range of 15°–30°. It should be noted that figure 8 does not address any effects due to volatility.

Experiments were then conducted using the experimental configuration discussed above where two types of coal dusts with identical size distributions, but with volatilities of 36.1 and 17.2%, were dispersed and the angular intensities measured using the first scattering module described previously. Subsequently, additional tests were conducted where coal dusts of unknown size distribution and volatility were dispersed. The results of these experiments, obtained for respirable coal dust concentrations in the range of 1–12 mg m^{-3}, showed that the intensities per unit mass are constant at both 15° and 22.5°, but at 30° and 45° the intensities per unit mass begin to differ, and at 45°, this difference is in the range of 20–30%. These results are in excellent agreement with the results predicted from the theoretical analysis, where at a $\lambda = 600$ nm, the optimum angle for measurement was found to lie in the range of 15°–20°. For the two coal dusts of known volatility and size distribution, the angular intensity distributions were computed, normalized to the value at 15°, and then compared to the data. The results are shown in figure 9 for the two different coal dusts. For each of the dusts, there two theoretical curves are shown. These two

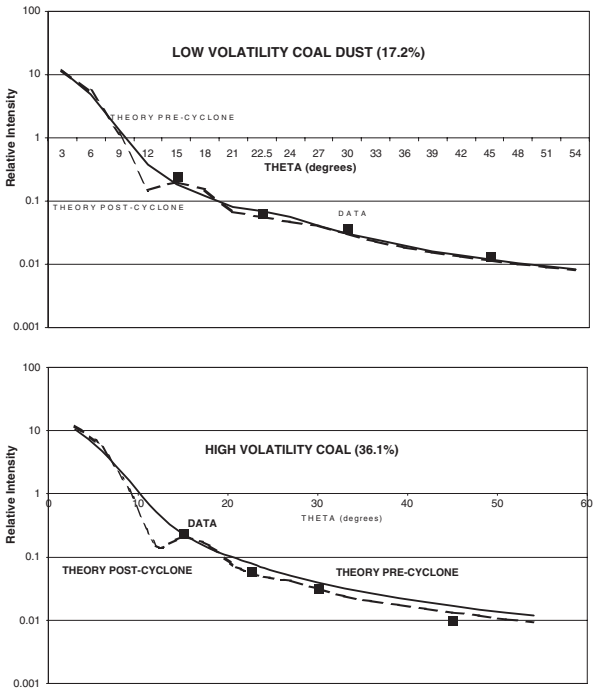

Figure 9. Measured and predicted angular intensities for two coals of uniform particle size distribution, but differing in volatility by more than a factor of 2.

curves correspond to the dust particle size distribution measured prior to the experiments and the calculated size distribution after passage through the 10 mm cyclone. The net effect of passage through the cyclone is to reduce the number of larger particles that pass through the cyclone more drastically than the smaller particles, thus resulting in a smaller mass mean diameter and a much narrower distribution. For the as-received dusts, the measured distributions had a mass mean diameter of 5.7 μm and a σ of 1.45. After passage through the cyclone, the mass mean diameter was calculated to be 3.75 μm with a σ equal to 1.15. The theoretical intensity distributions were then calculated for each of these distributions. The agreement between theory and experiment is very good, in spite of the fact that the theoretical computation assumes perfectly spherical particles when in reality dust particles have quite irregular shapes.

3.2. DPM

While it was not the specific intent of this research to study the angular intensity distributions in any great detail, the general differences between respirable coal dust and DPM are worth noting. Several experiments were conducted where DPM was dispersed and the angular intensities measured. For DPM, attempts were made to use the Mie scattering algorithm to arrive at some set of size distribution parameters (d_M and σ) that reasonably approximated the angular intensity distribution measured, but these attempts produced unrealistic results. Previous research [8] had shown that the angular intensity distribution for DPM could be more accurately described by treating DPM as fractal-like aggregates with angular intensity distributions defined by the Fisher–Buford expression [11]

$$I(q)/I(0) = (1 + 2q^2 R_G^2/3D)^{-D/2} \qquad (9)$$

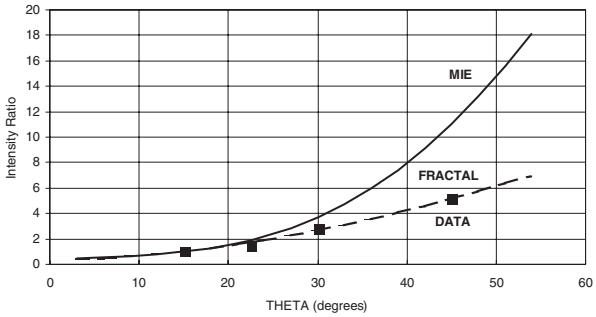

Figure 10. The measured angular intensity ratios for DPM compared with the ratios predicted from both the classical Mie theory and the fractal theory.

where q is the scattering vector defined by $q = (4\pi/\lambda)\sin(\theta/2)$ at the scattering angle θ, D is the fractal, or Hausdorff dimension and R_G is the radius of gyration (μm).

The results for a typical experiment conducted in the dust box at a DPM mass concentration of 2.9 mg m^{-3} are shown in figure 10, where the values of D and R_G that provide the best fit to the data are 1.85 and 0.865 μm, respectively. For comparison, the results of the Mie calculation are also shown, using $d_M = 2R_G$, $\sigma = 1.70$, and the index of refraction, $m = 1.68 - 1.06$i from [8]. This value of D is slightly greater than the value of 1.77 previously reported, while the value of R_G is almost a factor of 2 greater than the previously reported value of 0.48 μm. The difference in D is probably within the range of experimental error, while the more significant difference in R_G can be attributed to the much longer aging time of the particles prior to measurement.

3.3. DPM and respirable coal dust

Subsequently, another series of tests were conducted where DPM, respirable coal dust and mixtures of the two were dispersed at DPM concentrations in the range of 2–8 mg m^{-3}, respirable coal dust concentrations in the range of 6–11 mg m^{-3} and various mixtures of the two at total concentrations typically around 11–13 mg m^{-3}. Measurements were made using the first scattering module and the second, unipolar ion chamber described previously. In general, these data indicated that the intensities per unit mass for DPM were lower than those of respirable coal. Figure 11 is a plot of the average intensities measured at 15° for pure DPM, pure respirable coal dust and mixtures of the two. For pure DPM, the average intensity per unit mass is in the range of 0.022 V (mg/m^3)$^{-1}$, while for pure respirable coal dust, the intensity per unit mass is around 0.065 V (mg/m^3)$^{-1}$. Perhaps of greater significance are the angular intensity ratios for the two types of particles. These ratios are shown in table 1. It should be noted that these ratios are averages of the raw data, uncorrected for differences in the angular scattering volumes.

These data would indicate that the intensity for respirable coal dust decreases rapidly as the angle increases, while for DPM the intensity decrease is more gradual. These ratios were also measured for mixtures of DPM and respirable coal dust, where the ratios $I_1(15)/I_1(30)$ and $I_1(15)/I_1(45)$ were found to decrease linearly as the mass fraction of DPM increased from 0 to 1. These results are shown in figure 12, and indicate that

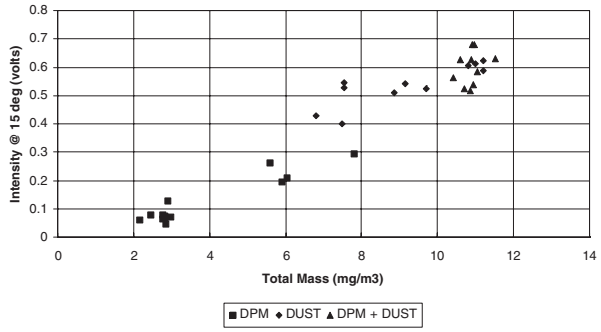

Figure 11. Angular intensity measured at 15°, expressed in volts, for respirable coal dust, DPM, and mixtures of DPM and respirable coal dust for the first scattering module.

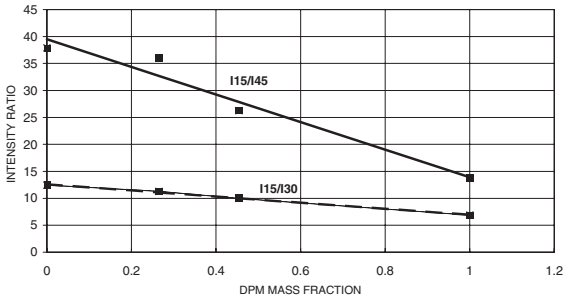

Figure 12. Angular intensity ratios measured for respirable coal dust, DPM, and mixtures of DPM and respirable coal dust using the first scattering module.

Table 1. Average angular intensity ratios measured for pure concentrations of DPM and pure concentrations of respirable coal dust.

Ratio	DPM	Dust
$I_1(15)/I_1(22\frac{1}{2})$	2.36	3.14
$I_1(15)/I_1(30)$	6.45	11.82
$I_1(15)/I_1(45)$	13.76	37.90

when DPM/dust mixtures exist, a determination of one of these ratios could be used to estimate the relative mass fractions of the two components. However, considering that the allowable time-weighted average concentration of DPM is a factor of 10 lower than that for dust, this determination could have limited applicability, especially in mixtures where DPM is less than or equal to about 10% of the total mixture. Determination of one of these ratios could be used as a check of some other measurement, or combination of measurements, to increase the reliability of the data, and the inferred mass measurements. This application would imply that separate methods should exist for determination of DPM and respirable coal dust.

To address this possibility, and actually as an afterthought, the particles exiting the scattering module were diverted into the unipolar ion chamber described previously, where the parameter, η, defined in equation (3), was measured. For DPM, the change in η was significant, as was expected. When subjected to pure respirable coal dust, there was no discernible change in η, even for dust concentrations in the range of 11–12 mg m^{-3}. Additional measurements were made using various mixtures of DPM/dust. For these measurements, the change in η was found to depend *only* upon the DPM concentration. In addition, the ion chamber sensitivity, expressed as the change in η divided by the change in mass concentration of DPM, or $\Delta\eta/\Delta m_{\mathrm{DPM}}$, for pure DPM remained constant for the DPM/dust mixtures. The results of these experiments are shown in figure 13, where the quantity, $1-\eta$, is plotted as a function of the DPM mass concentration for pure DPM, pure respirable coal dust, and mixtures of the two. These results implied that a simple two-component measuring device has significant potential for measurement of DPM independent of respirable coal dust, and vice versa.

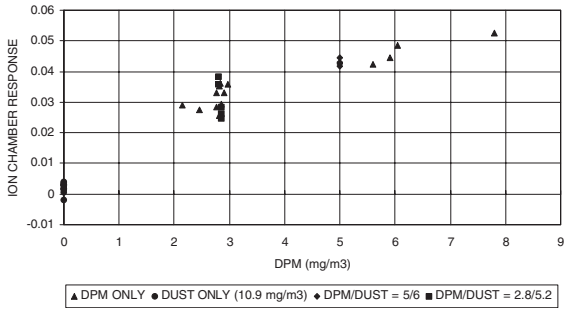

Figure 13. The current loss ratio parameter, $1-\eta$, measured for respirable coal dust, DPM, and mixtures of DPM and respirable coal dust using the second, unipolar, ion chamber.

The light-scattering component of the device was described previously (figure 3), as was the ion chamber (figure 4). These two components were subsequently evaluated in another series of experiments. In these experiments pure respirable coal dust was dispersed at mass concentrations in the range of 1.0–4.5 mg m^{-3}. The results of approximately 25 measurements yielded sensitivities, expressed as the change in intensity divided by the change in respirable dust mass concentration, $\Delta I_2(15)/\Delta m_{\mathrm{DUST}}$ and $\Delta I_2(30)/\Delta m_{\mathrm{DUST}}$, of 0.113 V (mg/m^3)$^{-1}$ ±2.5% and 0.032 V (mg/m^3)$^{-1}$ ± 6%, respectively. These values are significantly higher than those previously obtained using the first scattering module, where the values were $\Delta I_1(15)/\Delta m_{\mathrm{DUST}} = 0.065$ and $\Delta I_1(30)/\Delta m_{\mathrm{DUST}} = 0.0055$. Similarly, the scattering ratio for the second scattering module, $I_2(15)/I_2(30)$, is 3.53, compared with a value of $I_1(15)/I_1(30) = 11.8$ measured using the first scattering module. It is felt that the differences between the two light-scattering modules are due to differences in the light source beams used in the modules, and some additional studies are being undertaken to reconcile these differences.

Following these tests, DPM was then dispersed at concentrations from 0 to about 3.0 mg m^{-3}. For these tests, the average sensitivities for angular scattering were measured to be $\Delta I_2(15)/\Delta m_{\mathrm{DPM}} = 0.064$ V (mg/m^3)$^{-1}$ ± 10.5% and $\Delta I_2(30)/\Delta m_{\mathrm{DPM}} = 0.0314 \pm 11.2\%$. While there is more uncertainty in the sensitivity at each angle for DPM compared with the respirable coal dust, it is worth noting that the intensity ratio, $I_2(15)/I_2(30)$, was much more stable with an average value of 2.04 ± 1.5%. Also worth noting, is the fact that this ratio is also considerably less than the ratio obtained with the first scattering module ($I_1(15)/I_1(30) = 6.45$), a result similar to that found for respirable coal dust. An analysis of these data would indicate that the difference in intensities at the two angles (i.e. the slope) is sufficiently different to allow for determination of whether the particles are DPM or respirable coal

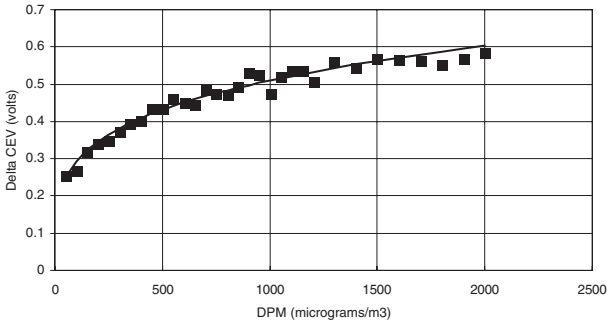

Figure 14. The measured change in floating electrode potential, ΔCEV, as a function of DPM mass concentration, using the first, bipolar, ion chamber.

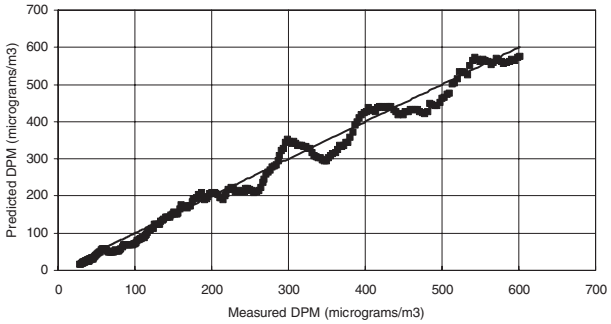

Figure 15. A comparison of the predicted and measured DPM mass concentrations using the empirical equation (9) over the concentration range of 25–600 μg m^{-3}.

dust. For DPM, this difference is 0.0326 V $(\mathrm{mg/m^3})^{-1}$, while for respirable coal dust the difference is 0.081 V $(\mathrm{mg/m^3})^{-1}$, a factor of 2.5 greater.

In addition to the light-scattering data, data were also acquired using the bipolar ion chamber. For respirable coal dust, there was no response, as previously observed using the unipolar ion chamber. For DPM, the change in potential of the floating, collection electrode was found to increase rapidly at low concentrations ($\leqslant$0.50 mg m^{-3}) and then to decrease more slowly as the DPM mass concentration increased further. Figure 14 is a plot of the change in the voltage at the collection electrode (CEV) as a function of the mass concentration of DPM, spanning the range from zero to 2.0 mg m^{-3}, where these changes are readily apparent. Throughout the mass range, the following empirical expression (full curve of figure 14) was found to adequately describe ΔCEV as a function of DPM mass concentration

$$\Delta\mathrm{CEV} = 0.51(m_{\mathrm{DPM}})^{0.242}. \tag{10}$$

Of particular interest is the concentration range from 50 to 200 μg m^{-3}, since this is the range (and greater) over which DPM measurements will be required. Within this range, the empirical expression, defined by equation (10), predicts the measured values to within ±5%. To demonstrate the utility of this expression, equation (10) is rearranged as

$$m_{\mathrm{DPM}} = (\Delta\mathrm{CEV}/0.51)^{4.1322} \tag{11}$$

so that the predicted mass of DPM can be determined from the measured CEV. A plot of the predicted versus measured DPM mass concentrations is shown in figure 15 over the concentration range of 25–600 μg m^{-3}, where the full line is the line of perfect agreement.

Although there are some deviations between predicted and measured values, it is felt that some of these variations may, in fact, be real variations, and not 'noise' related to the ion chamber. However, the accuracy with which a determination of the DPM mass concentration can be made is dependent upon the signal to noise ratio (SNR) of the ion chamber. To address this potential problem, separate tests were conducted during which the steady-state CEV was monitored for extended periods of time and measurements made once every 2 s. These data were then averaged over discrete time intervals up to 120 s (60 measurements) to determine if time averaging could reduce the electronic noise of the ion chamber. For a total time period of 60 min (3600 s, or 1800 measurements), the average steady-state CEV was 3.416 with a standard deviation of ±0.015 726 V. From equation (10), at a mass concentration of 100 μg m^{-3}, the change in CEV is 0.292 126 V. At one standard deviation lower, 0.2764 V, the calculated mass concentration would be 79.6 μg m^{-3}, while at one standard deviation higher, 0.307 852 V, the calculated mass concentration would be 124.2 μg m^{-3}. If the measurements are averaged over a time interval of 60 s, then the standard deviation is reduced to ±0.003 378 V. Using this value as the uncertainty in the measurement, the lower and upper calculated mass concentrations would be 95.3 and 104.9 μg m^{-3} respectively. The use of signal averaging reduces the uncertainty in the mass determination from ±24% to ±5%.

4. Conclusions

The data and analyses presented for these two types of particles relative to monitoring for health purposes are clear and unequivocal. Angular light scattering at one or at most two angles in the range of 15°–30°, using a simple light-scattering module similar, or identical, to the one described as the second scattering module, can provide a determination of the mass concentration of respirable coal dusts with a high degree of accuracy only minimally influenced by particle size or chemical composition. Both the theory and the experiments confirm this conclusion. For DPM, the bipolar ion chamber provides a simple, low-cost device of high sensitivity and selectivity. For mixtures of DPM and respirable coal dust, the combination of these two devices can provide for determination of the individual mass concentrations of each component. Prototypes embodying these two techniques should be fabricated for subsequent testing and evaluation in underground mines or within other workplaces where similar needs exist.

References

[1] Title 30 1995 *US Code of Federal Regulations* Part 70.100 July, 1995 p 413

[2] Cassinelli M E and O'Connor P F (ed) 1994 *NIOSH Manual of Analytic Methods* 4th edn (DHHS (NIOSH) Publication) pp 94–113

[3] Scherrer H C, Kittelson D B and Dolan D F 1982 Light absorption measurements of diesel particulate matter *Society of Automotive Engineers Paper* 810181 p 7

[4] Volkwein J C, Schoeneman A L and Page S J 2000 Laboratory evaluation of pressure differential based respirable dust detector tube *Appl. Occup. Environ. Hyg.* **15** 158–64

[5] Marple V A, Kittelson D B, Rubow K L and Fang C P 1986 Methods for the selective sampling of diesel particulate in mine dust aerosols *Final Report Contract* J0145022 (University of Minnesota) p 94

[6] Patashnick H and Rupprecht G 1986 Microweighing goes on-line in real time *Res. Dev.* **28** 74–78

[7] Barber P W and Hill S C 1990 *Light Scattering by Particles: Computational Methods* (Singapore: World Scientific)

[8] Litton C D 1997 Fractal properties of smoke produced from smoldering and flaming fires *Proc. ASME* **352** 119–34

[9] Sorensen C M and Feke G D 1995 *ICFRE: Post-Flame Soot Proc. Int. Conf. Fire Research and Engineering (Orlando, FL, Sept. 1995)* pp 281–5

[10] Dobbins R A, Mulholland G W and Bryner N P 1994 Comparison of a fractal smoke optics model with light extinction measurements *Atmos. Environ.* **28** 889–97

[11] Sorensen C M 2001 Light scattering by fractal aggregates: a review *Aerosol Sci. Technol.* **35** 648–87

[12] Marple V A and Rubow K L 1983 An Aerosol chamber for instrument evaluation and calibration *Am. Ind. Hyg. Assoc. J.* **44** 361–7

[13] Cannon C G and George H W 1943 *Proc. Conf. on the Ultra-Fine Structure of Coals and Cokes (London)* (London: British Coal Utilization Research Association) pp 290–316

[14] McCartney J T and Ergun S 1967 Optical properties of coals and graphite *US Bureau Mines Bull.* **641** p 49

[15] Litton C D 1977 A mathematical model for ionization-type smoke detectors and the reduced source approximation *Fire Technol.* **13** 266–81